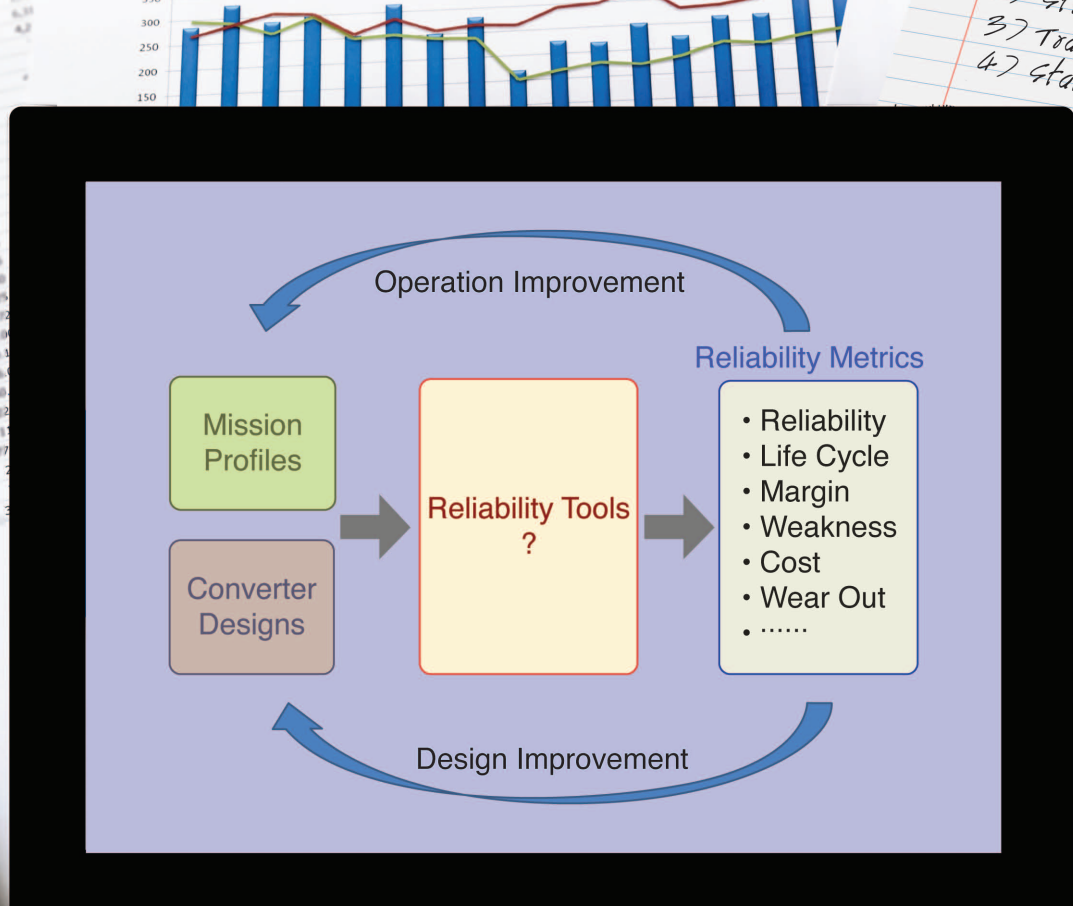


New Approaches to Reliability Assessment

Using physics-of-failure for prediction and design in power electronics systems

by Ke Ma, Huai Wang, and Frede Blaabjerg



Power electronics are facing continuous pressure to be cheaper and smaller, have a higher power density, and, in some cases, also operate at higher temperatures. At the same time, power electronics products are expected to have reduced failures because it is essential for reducing the cost of energy. New approaches for reliability assessment are being taken in the design phase of power electronics systems based on the physics-of-failure in components. In this approach, many new methods, such as multidisciplinary simulation tools, strength testing of components, translation of mission profiles, and statistical analysis, are involved to enable better prediction and design of reliability for products. This article gives an overview of the new design flow in the reliability engineering of power electronics from the system-level point of view and discusses some of the emerging needs for the technology in this field.

Reliability Metrics in Power Electronics

Modern society needs to become more energy efficient and use more renewable generation to be sustainable. A key technology in this mission is power electronics, which convert electrical energy from one stage to another. In past decades, power electronics have been widely installed in emerging energy conversion applications, such as renewables, motor drives, aircraft, power quality/transmission, etc. The fast growth on the installed capacity makes the failures of the power electronics system costly—due not only to the increased maintenance and repair but also to the adverse impacts to other systems and loss of energy commitments [1]–[6]. On the other hand, there has been continuous pressure for power electronics manufacturers to reduce costs and keep their products competitive on the market. To satisfy the stringent reliability requirements while limiting the cost and development/testing time, there is strong demand for more accurate evaluation and design of reliability performance for power electronics converters.

Different from the conventional performance metrics for power electronics, such as efficiency, power density, total harmonics distortion, etc., reliability is a performance that is difficult to quantify and measure. In the past, most reliability information for power electronics was collected at the component level from the statistics of failed products, and then experience-based handbooks were established as a foundation to predict the lifetime of the whole converter system [1]. This approach has proven to be inaccurate as it is application independent, providing no clues for the root cause of failures or for design improvement. Research on power electronics reliability has advanced in the last decades. However, an understanding of the fundamental failure mechanisms of the power electronic components, the impact on the reliability affected by multiphysical stressors (e.g., temperature, humidity, vibration, cosmic radiation, etc.), and the interactions among them during operation is still lacking. Moreover, the modeling of the impact and the need for a breakthrough in time-efficient reliability verification methods, coupled with demand from industry to reduce development costs, are great scientific challenges.

A more advanced approach to predict the reliability of power electronics is shown in Figure 1. In this method, a series of reliability tools are expected to be established and can be used to transfer the mission profiles (i.e., the operating condition and environment of the system), as well as the given converter designs, to a series of quantified reliability metrics defined in the field of reliability engineering. In this approach, the applications of converter and reliability performance are closely correlated, making it possible to accurately improve and verify the design or operation of converters to achieve certain reliability specifications before they are introduced into the market—this feature is significantly useful for power electronic system manufacturers in reducing cost.

The Reliability Metrics for Power Electronics

The engineering definition of *reliability* is the probability that an item will perform a required function without failure under stated conditions for a specified period of time [2].

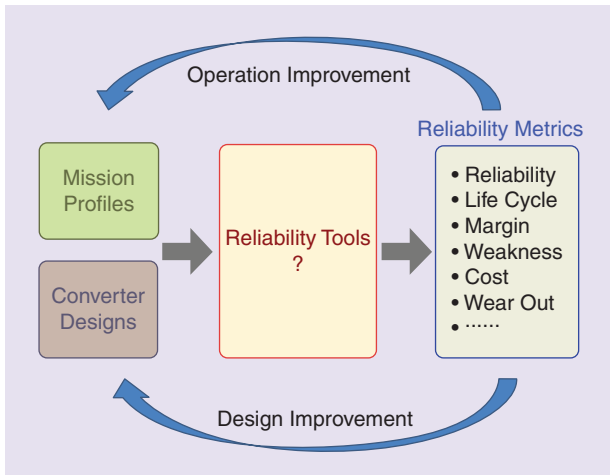


FIG 1 An advanced approach for the reliability prediction of a power electronics system.

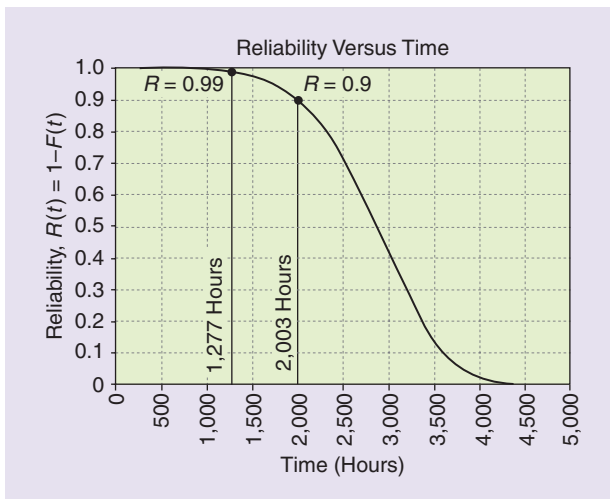


FIG 2 An example of reliability and percentile lifetime of a type of 1,100-V/40- μ F film capacitors under 85 °C and 85% RH with a 5% capacitance drop as the end-of-life criteria [3]. $R(t)$: reliability with time; $F(t)$: unreliability.

Accordingly, a comprehensive reliability description includes five important aspects: definition of failure criteria, stress condition, reliability numbers (%), confidence level (%), and the time of interest. A reliability number can vary by adjusting any one of the other four aspects. Understanding the metrics used in reliability engineering is a fundamental step for the assessment of reliability performance and to be able to set the modeling targets. In the following, several important concepts and definitions are first clarified.

Reliability, Failure Rates, Mean Time to Failure, and Lifetime
To quantify reliability from a reliability engineering perspective, a time-varying variable $R(t)$ as a percentage is used and represents the percentage of a group of samples that can properly function at a certain time t . From the point of view of individual sample, $R(t)$ can be also represented as the prob-

ability of one sample that can function at a certain time. Similarly, the unreliability $F(t)$ can be defined as percentage of a group of samples (or probability of one sample) that fail at a certain time t .

$F(t)$ can simply be calculated from $1 - R(t)$. The plot of $F(t)$ against time t is also referred to as the *cumulative distribution function (CDF)* curve, which in most cases can be fitted by an analytical function with three parameters γ , β , and η developed by Waloddi Weibull in 1951 [4], as shown in (1)

$$F(t) = 1 - \exp\left[-\left(\frac{t-\gamma}{\eta}\right)^\beta\right]. \quad (1)$$

The widely used term *mean time to failure (MTTF)* represents the average time that a group of samples fails. It is generally used in some reliability standards and handbooks for military and aerospace applications. The MTTF can be deduced from the reliability function $F(t)$ by (2). It is worth mentioning that the MTTF is an oversimplified term, which is independent of time and loses the whole picture of the reliability performance, such as failure distribution and hazard rate. Therefore, benchmarking the systems or components by using MTTF is discouraged if the reliability function or CDF curve can be generated [1]–[3].

$$\text{MTTF} = \int_0^{\infty} R(t) dt. \quad (2)$$

To better quantify the lifetime of the system or component, percentile lifetime B_x is more suitable and recommended for use. It is the time when a group of samples has a certain percentage of failure. For example, a B10 lifetime corresponds to the time at which 10% of the samples in a group have failed or the time at which a testing sample has 10% probability of failure. The percentile lifetime can easily be solved from the reliability function or CDF curve, and the time-varying characteristic of failure is still kept. Figure 2 describes the relationship between the reliability and percentile life based on an example of film capacitors. The B1 lifetime ($R = 0.99$) and B10 lifetime ($R = 0.9$) in the example are 1,277 and 2,003 hours, respectively.

The failure rate $\lambda(t)$ [also called *hazard rate* $h(t)$] is another important reliability metric widely used in reliability engineering. It describes the frequency with which a system or component fails. It can be expressed in failures per unit of time by deducting the reliability function $R(t)$ as

$$\lambda(t) = \frac{1}{R(t)} \frac{d[1-R(t)]}{dt}. \quad (3)$$

A typical failure rate curve against the time in the life cycle of a power electronics product is plotted in Figure 3. It is composed of three reliability functions and is known as the *bathtub curve* [2]. By examining the fitting parameters β in the reliability functions, three types of failures that are dominant at different stages of the life cycle can be identified. The first part is dominated by early failures caused by infant mortality, with a decreasing failure rate (where

$\beta < 1$). The second part is dominated by random failures in the useful life of a product, with a constant failure rate (where $\beta = 1$). The third part is dominated by wear-out failures in the end of life of the product, with an increasing failure rate (where $\beta > 1$).

The reliability/unreliability function (or CDF curve) provides a clear picture of the probability of failure as well as the characteristics of failures developing with time. By this function, many other reliability metrics can be deduced. The early failure shown in Figure 3 is more related to the production capability of a manufacturer, while the failures in the useful life of a product are more related to random events/usages. These two types of failures are normally difficult to model and predict.

Mission Profiles

The mission profiles indicate the operating conditions and functions that a power electronics converter needs to perform during its specified life cycle. Typical mission profiles for power electronics could be defined as, e.g., the wind speed/solar irradiance (for the renewable energy production), speed and torque variations of the electric machine (for the motor drive application), the operational ranges/codes for the output voltage/current, the usage behaviors of customers, and also the environmental factors like temperature, humidity, vibration level, etc. The mission profiles are closely related to the stress/loading of the components, which is the main source of the failures in the power electronics components. Meanwhile, the mission profiles will lead to various design solutions for the converter and have a strong impact on the cost of products. As a result, understanding the mission profiles is also a fundamental step for the reliability analysis of power electronics.

New Approach to Assess the Reliability Metrics of Power Electronics

Assessing the reliability metrics of a converter system, which contains many different kinds of components with complex operating/loading conditions, is still a challenging task. Today, most reliability information of power electronics components has to be collected by statistical analysis of failed products [7]–[11], and then experience-based handbooks are established as guidance to determine the lifetime of different devices and designs. This approach has been proven inaccurate, as it is too general and application independent. An alternative method for assessing the reliability metrics of a converter is shown in Figure 4 [6], which separates the problem into four different groups of research/modeling activities. In this structure, the critical components, as well as the major failure mechanisms, in a converter system need first to be filtered out and identified. Based on the interested failure mechanisms in the critical components, the stress experienced by these components is translated from the given mission profiles and design solution of a converter. On the other hand, the reliability of the interested components under different stress levels in practical use is tested and modeled to

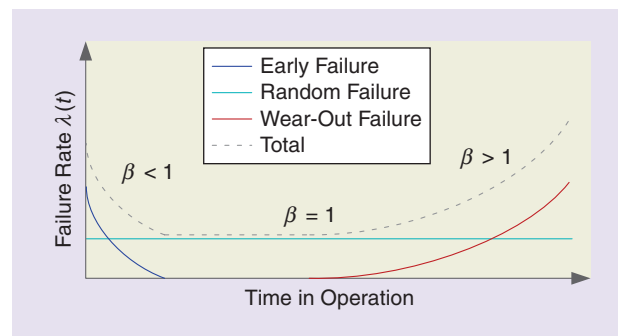


FIG 3 The bathtub curve, or failure rate, in the life cycle of a typical power electronics product.

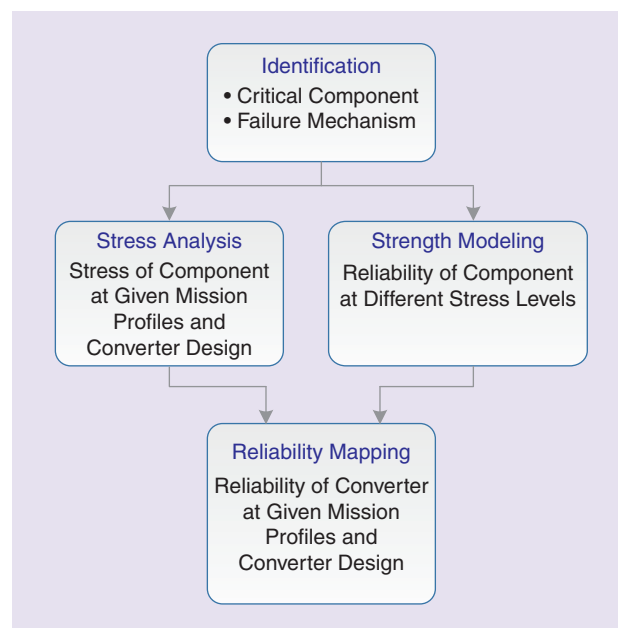


FIG 4 Analysis flow for assessing the reliability metrics of a power electronics converter [6].

reflect the strength information of the components. Finally, a series of algorithms and statistical analysis is introduced to map the overall reliability metrics of the whole converter system under the given mission profiles and design solutions. The potential methodologies in the four different activities in Figure 4 are briefly discussed later.

Identification of Critical Components and Failure Mechanism

Understanding of the reliability physics of power electronic components is a starting point to assess reliability of the converter system. The target of this group of analyses is to identify the most critical components/assemblies in a system and then the major failure mechanisms, as well as the corresponding stressors, which trigger the failure of components. This information normally has to rely on the investigations and statistics based on the failed products/components in the field. Various investigations have been done into the failure causes and distributions in power electronics systems

Table 1. The FPM in reliability of power electronic components [1].

Load			Focus Points									
Climate + Design ≥ Stressor			Active Power Components			Passive Power Components		Control Circuitry, IC, PCB, Connectors				
Ambient	Product Design	Stressors	Die	LASJ	Wire bond	Cap.	Ind.	Solder Joint	MLCC	IC	PCB	Connectors
Temperature —T(t)	—Thermal system	Temperature swing ΔT	X	X	X			X				
	—Operation point	Average temperature T	X	X	X	X		X	X	X	X	X
	—ON/OFF power P(t)	dT/dt	x	x	x	x						
		Water								X	X	X
		Relative humidity	x	x	x	X	X	x	x	X	X	X
Pollution	Tightness	Pollution						X				X
Mains	Circuit	Voltage	x	x	x	X	X		x	x	x	x
Cosmic	Circuit	Voltage	x									
Mounting	Mechanical	Chock/vibration	x			x	x	x	x			x

LASJ: large-area solder joint; MLCC: multilayer ceramic capacitor; IC: integrated circuit; Cap.: capacitor; Ind.: inductor. Level of importance (from high to low): X-X-X-x.

[7]–[11]. However, it is continuously challenged as new materials and devices are appearing on the market.

In a typical power electronic system, power semiconductor devices, capacitors, gate drivers, connectors, printed circuit boards (PCBs), and fans are considered as the vulnerable components, especially the insulated-gate bipolar transistor (IGBT) modules in medium- to high-power applications and capacitors for ac filtering and dc-link applications. A focus point matrix (FPM) was presented in [1] to show the critical stressors for different components, which are represented in Table 1. The steady-state temperature, temperature swings, humidity, voltage, and vibrations have different levels of impact on semiconductor devices, capacitors, inductors, and low-power control boards.

As two of the most vulnerable power electronics components with respect to reliability, the failure mechanisms of IGBT modules and capacitors are surveyed in [12] and [13], respectively. Thermal cycling (i.e., temperature swings inside or outside the devices) is one of the most critical stressors in power electronics components [10], [11], [14], [15]. It is widely accepted that the temperature fluctuation on different materials with mismatched coefficients of thermal expansion may cause disconnection at the material boundaries, thus leading to wear-out failures of the devices. Similarly, it has been found that the thermal-related failures also exist in the capacitor and PCB, and they are claimed to be one of the most important root causes of failures in these power electronics components [10]. Different types of capacitors, such as electrolytic capacitors, film capacitors, and ceramic capacitors, also have thermal-related failure

mechanisms. The degradation of electrolytic capacitors is temperature and voltage dependent. Besides these two critical stressors, humidity and vibration are critical to film capacitors and ceramic capacitors, respectively. The reliability of these capacitors for dc-link applications is discussed in [13] in detail.

Stress Analysis and Translation from Mission Profiles

After the reliability-critical components and the major failure mechanisms are identified for a power electronics system, the major stress of the components can be comprehensively evaluated by modeling the loading conditions in a specific application with a given converter design. The target of this group of analyses is to establish models that can translate the mission profiles and converter design to the quantified stresses that will trigger the failure of devices under a failure mechanism.

Challenges of Mission Profiles Translation

The correct modeling of stress in power electronics components could be a challenging task. As previously mentioned, the device loadings are closely related to the mission profiles of the whole converter system, which includes complicated models not only for the electrical system but also for environmental conditions and the mechanical system. The typical signal flows and model block diagram to assess the thermal stress of power electronics components in a grid-tied inverter are illustrated in Figure 5, where the disturbances, feedback loops, and relationship between physical domains can be identified [16]. When translating the mission profiles to the stress of components, multidisciplinary models have to be involved with different analyzing methods

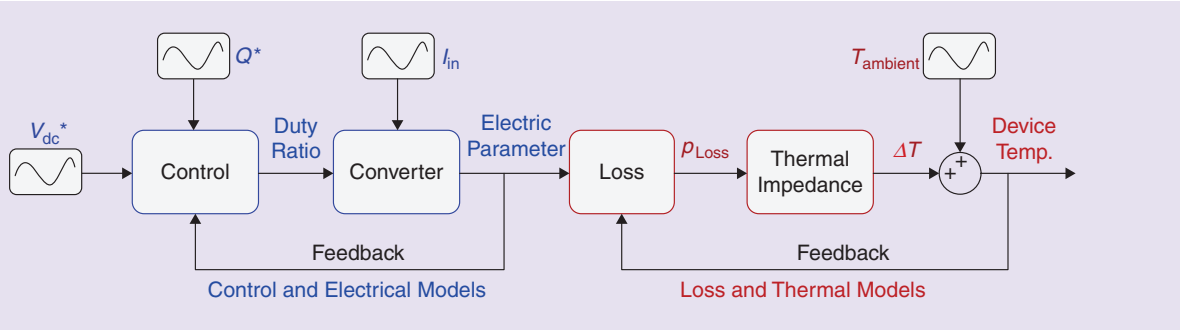


FIG 5 The typical signal flows and model block diagram to assess the thermal stress of power electronics components in a grid-tied inverter [16]. V_{dc}^* : dc link voltage control reference; Q^* : reactive power reference; I_{in} : input current on the dc link; P_{Loss} : power loss on the device; ΔT : temperature variation of the device; $T_{ambient}$: ambient temperature.

and tools, and finding out the correct connection or interaction among the results from different physical domains is of great importance.

The major disturbances and dominant time constants of the factors in a wind power generation system—a typical application of power electronics—that have influence on the loading of power semiconductor devices are illustrated in Figure 6 [17]. These factors have very different time constants, ranging from microseconds (power semiconductor device switching) to years (ambient temperature changes).

Examples of different time scales of thermal loading on the chips inside the power semiconductor device are shown in Figures 7 and 8. In Figure 7, the simulation results of a 2-MW full-scale wind power converter with a 1,100-V dc input, 690-V root mean square (rms) output dc/ac three-phase two-level topology is provided. In Figure 8, the experimental results of a 10-kW power converter with a 600-V dc input, 380-V rms output dc/ac three-phase three-level topology is shown by using an infrared camera [17]. The loading conditions are illustrated under different time scales: first, at a one-year span with a 3-hour sampling time and, then, at a 0.2-second span with a 350-Hz sampling rate. It can be clearly seen that the behavior of the thermal cycling under different time scales is quite different. The longer-term thermal cycling in Figure 7 is quite unregulated and mainly caused by the variations of converting power, depending on the wind speeds and turbine/generator operating conditions, while the short-term thermal cycling in Figure 8 is more stable and mainly disturbed by the alternating of load current at the grid line frequency.

Multitime Scale Modeling Approaches

The existing methods/tools for the power electronics are not sufficient to model the complete stress behaviors in the power device driven by the mission profiles. Either very detailed and refined models/methods (such as finite element methods or PSpice circuit models) are used but restrained to a very limited time span and small time steps, or only steady-state conditions are focused on with compromised accuracy of certain important thermal dynamics.

To establish a more complete thermal behavior of the power devices according to the mission profile of the converter, newer approaches have to be used. A potential method is demonstrated in Figure 9 [17]. As lenses with different focus lengths are used in the photography, the

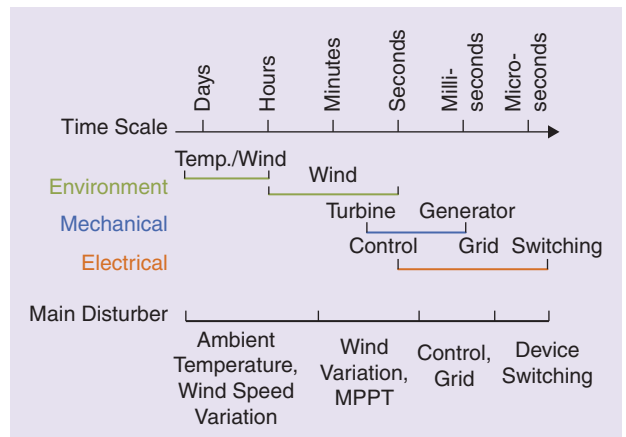


FIG 6 The multitime scale disturbances for the thermal behaviors in the wind power converter [17]. MPPT: maximum power point tracking.

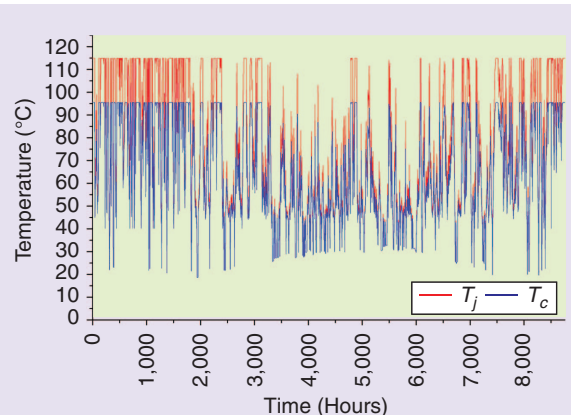


FIG 7 The simulation results of long-term thermal behaviors within one year with the temperature sampling rate at 3 hours (junction temperature T_j and case temperature T_c of the IGBT) [16].

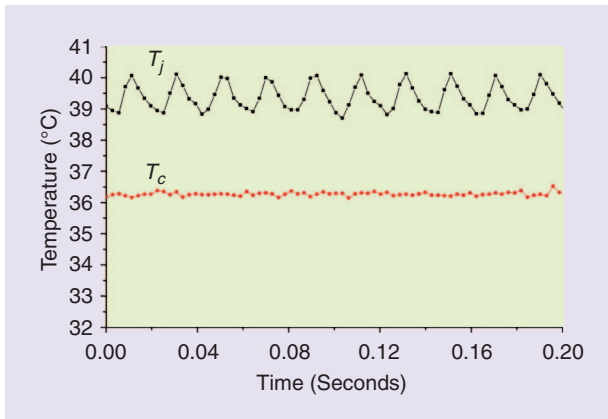


FIG 8 The experimental results of short-term thermal behaviors within 0.2 seconds with temperature sampling rate at 350 Hz (junction temperature T_J and case temperature T_c of the IGBT) [16].

loading analysis and modeling of the converter are separated under several time constants with different focuses and details of the systems. As an example, for the wind turbine application, three different modeling levels can be defined with different modeling techniques/tools [17]. Each of the modeling levels covers different aspects of the power converter from the component level to environmental level and thereby can correctly reflect different causes of thermal dynamics. More details of this multitime scale thermal modeling approach can be found in [18], and the interaction between different levels of modeling techniques was demonstrated in [19].

Another approach to handle the widespread time scales in the stress analysis of power electronics components is to establish frequency-domain models, which can transfer the various disturbances in the mission profiles to the dynamics stresses in the components regardless of the time scale. A frequency domain thermal impedance model for a power semiconductor device is thereby proposed for this purpose [20], as illustrated in Figure 10, in which a low-pass filter (LPF) is added to the thermal path. The new thermal impedance model can achieve more accurate modeling of the thermal dynamics of the power semiconductors at different locations from chips to the case and heat sink, which have quite different thermal dynamics and are difficult to be covered by the conventional modeling techniques.

Strength Testing and Modeling of Components

The target of this group of analyses is to test and model the reliability/lifetime of power electronics components under different stress levels, which is also referred as *reliability/lifetime models* of components. By knowing this critical information, the previously acquired component stress translated from the mission profiles can be mapped into the reliability of components under given mission profiles.

Accelerated testing is an important way to obtain component models of degradation, lifetime, and reliability or weak design points. Among various testing concepts, accelerated lifetime testing (ALT) [21], calibrated ALT (CALT) [22], multiple environment overstress tests (MEOST) [23], and highly accelerated limit testing (HALT) [24] have been

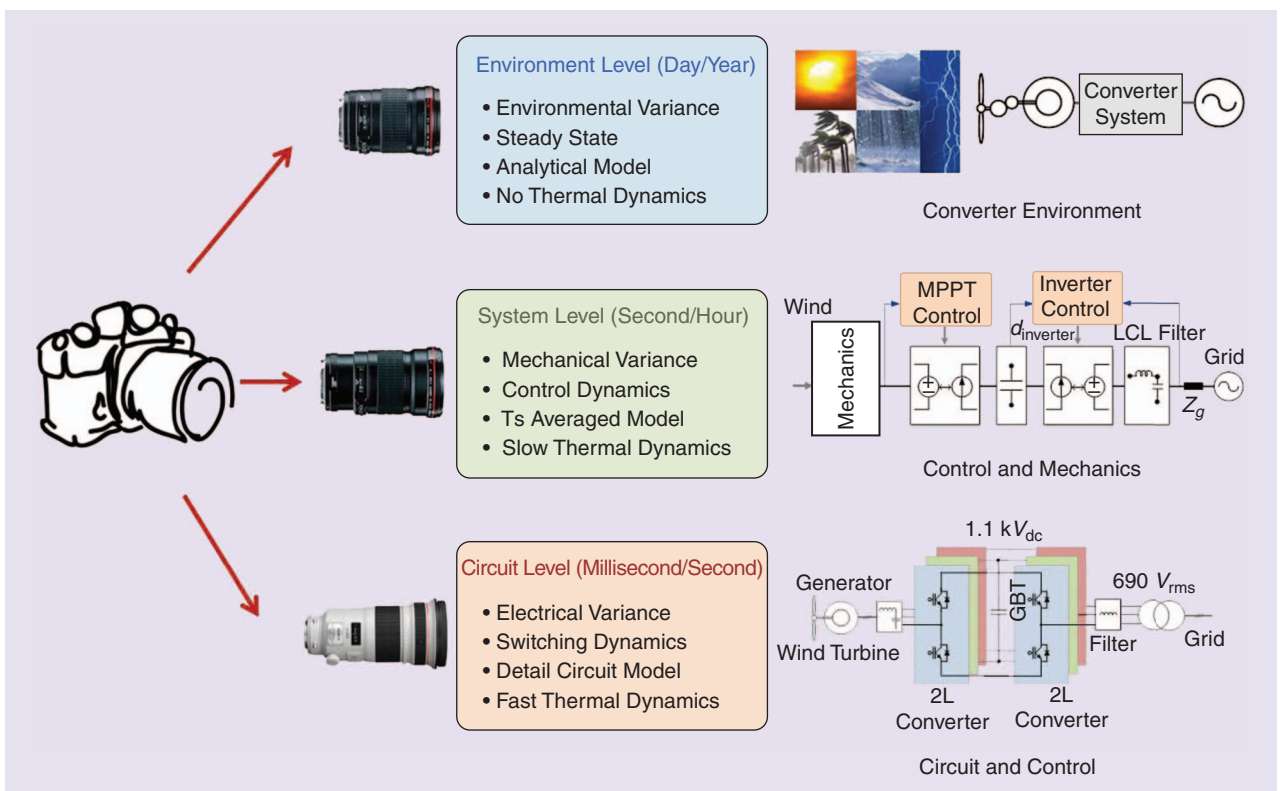


FIG 9 The multitime scale stress modeling approach of the power electronics converter in wind turbine generation.

widely studied and applied. The idea of ALT is to shorten the lifetime of an item by testing it at a higher stress level compared to that in the normal use. CALT and MEOST can be considered as two specific types of ALT. The stress levels of CALT are well calibrated according to the destruct limit and time budget, as discussed in [22]. MEOST puts emphasis on the failures due to interactions among multiple environmental and operational stressors. Different from the first three testing methods, HALT is a qualitative testing method at relatively higher stress levels, aiming to identify weak links or destruct limits, not to obtain quantitative models.

With respect to the application for power electronic components, it is a challenge to design an accelerated test with properly selected stressors and stress profiles, which have meaningful relevance to the practical field operation conditions. The pioneering work on the ALT of IGBT modules is presented in [25], [26] from the 1990s for traction applications. In [25], 300-A/1.2-kV IGBT modules from different suppliers are tested under different junction temperature variations ΔT_j within 30 °C and 80 °C, by circulating dc pulse currents. The heating time is between 0.6 and 4.8 seconds, focusing on the bond wire and chip solders related failure mechanisms. The study in [26] extends the investigations to baseplate solder joint reliability, also by including passive thermal cycling with a period of 4 minutes. Instead of using dc pulse currents, a more realistic current profile with pulselwidth modulation (PWM) switching is applied in [27] to test 600-V/200-A IGBT modules in automotive applications. The research efforts of power cycling testing of IGBT modules through 2014 are surveyed in [28] in terms of sample size, ΔT_j , and cycle period. In [29], the power cycling testing of 1.7-kV/1-kA IGBT modules in wind power applications was investigated with PWM switching current profiles, and real-time on-state saturation voltage monitoring. Recent work presented in [30] is devoted to studying the impact of the power cycling period on the cycle-to-failure of a type of IGBT module, where it turns out to be very important. ALT for capacitors and the corresponding lifetime models focus mainly on the impact of voltage and temperature stresses. As discussed in [13], humidity is also a critical stressor to film capacitors. To quantify the impact of humidity on the lifetime of film capacitors, a humidity-dependent model, where it turns out to be very

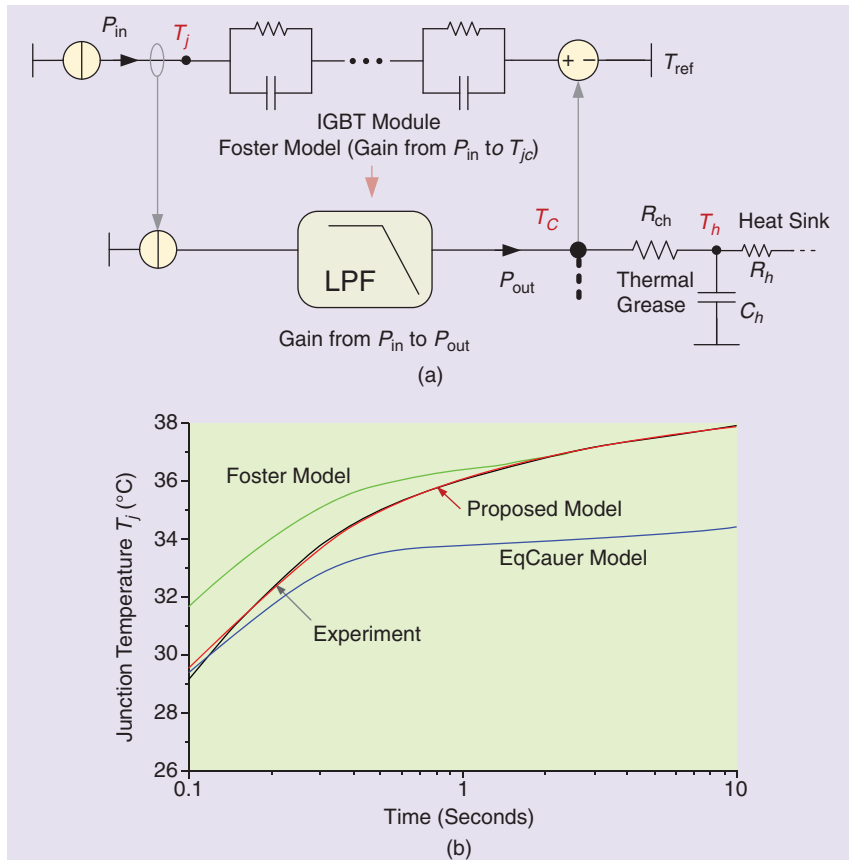


FIG 10 A frequency-domain thermal impedance model for power semiconductor devices [20].

important lifetime derating factor for dc film capacitors, is proposed based on ALT results as presented in [31]. The ALT of capacitors in [31] is represented later as an example to illustrate the testing procedure and testing data analysis methods.

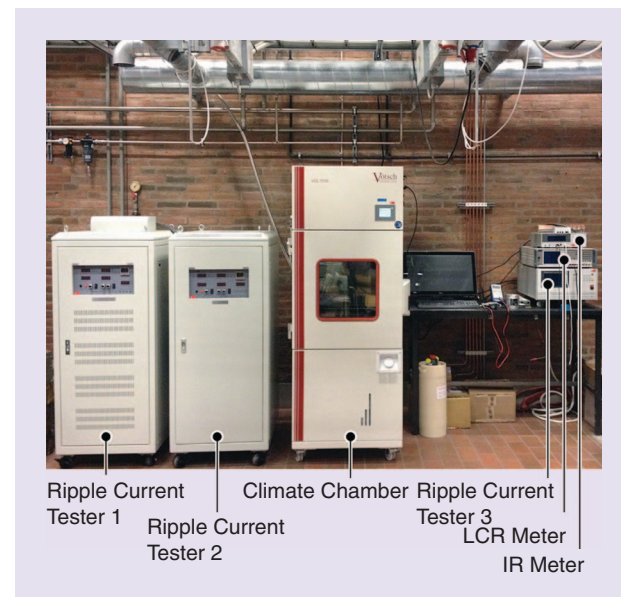


FIG 11 A capacitor degradation testing setup [31].

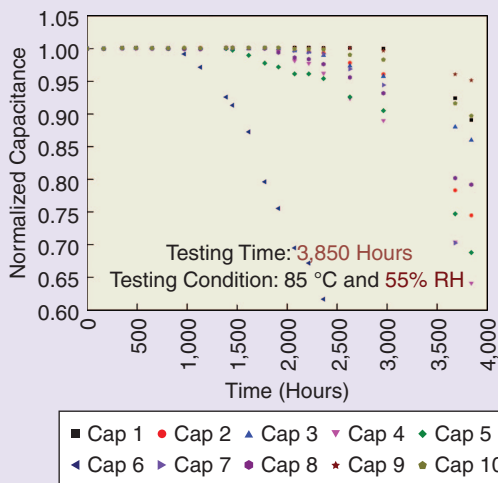


FIG 12 The normalized capacitances under 55% RH and 85 °C of ten capacitors (Cap) [31].

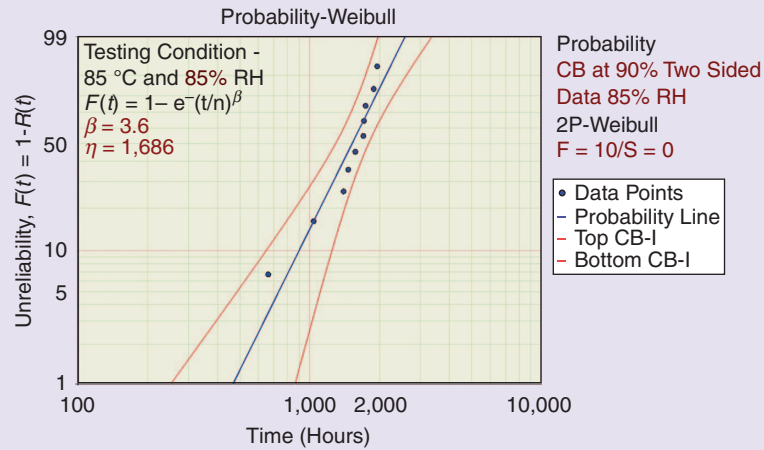


FIG 13 A Weibull plot of the testing results under 55% RH and 85 °C with 5% capacitance drop as the end-of-life criteria of ten capacitors [31].

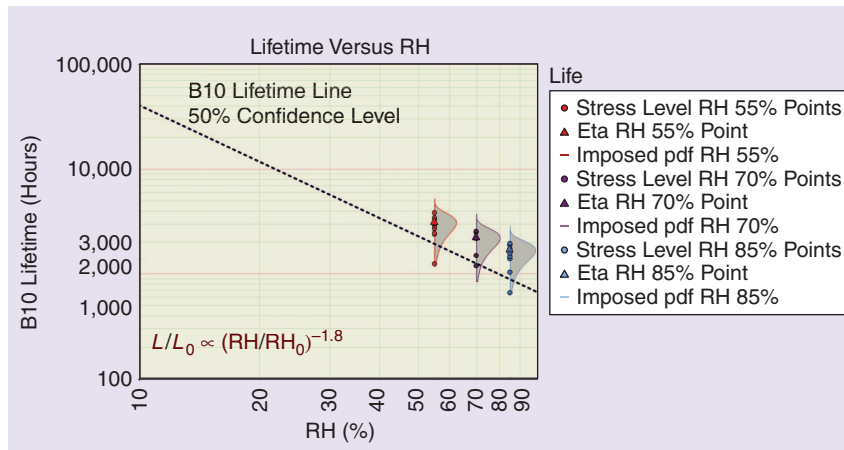


FIG 14 The B10 lifetime with 50% confidence level of the specific type of film capacitors versus RH levels under 85 °C and with 5% capacitance drop as the end-of-life criteria [31].

Table 2. Testing samples of metalized dc film capacitors [31].

Testing Samples	Testing Conditions
Group 1 – 1,100 V /40 μF (ten pieces)	85 °C and 85% RH
Group 2 – 1,100 V /40 μF (ten pieces)	85 °C and 70% RH
Group 3 – 1,100 V /40 μF (ten pieces)	85 °C and 55% RH

Figure 11 shows a capacitor testing setup. It is composed of a climatic chamber with a temperature range from -70 to 180 °C and a relative humidity (RH) level from 10 to 95% (within a certain temperature range); three ripple current testers to emulate electrical stresses of dc-link operation; an inductance, capacitance, and resistance (LCR) meter; and an insulation resistance (IR) and leakage current meter. The built-up system allows the testing of a wide range of film capacitors for the dc-link applications in power electronics. Specifically, for

the testing to be presented in this article, three groups of metalized film capacitors with the same part number for dc-link applications are investigated. The specifications and testing conditions of the capacitors are given in Table 2. The testing for Group 1, Group 2, and Group 3 lasts for 2,160, 2,700, and 3,850 hours, respectively. The ten samples in both Group 1 and Group 3 testing reach the end of life, with criteria of 5% of capacitance drop. As an example, Figures 12 and 13 show the measured normalized capacitance values (i.e., with respect to initial capacitance value) and the corresponding Weibull plot based on the results from Group 3 testing (see Table 2). According to the testing results, under the three different RH levels, a humidity-dependent B10 lifetime model is obtained as plotted in Figure 14, with an exponent constant of -1.8.

Figure 14 shows a typical lifetime model for the power electronics components (film capacitors), which reveals the relationship between the lifetime of the component (at a certain probability of failure) and the applied stress levels that will trigger a certain failure mechanism. Figure 15 shows another example of the power semiconductor from [25], in which the B10 lifetime (i.e., the number of cycles or time at which

the device has 10% probability of failure) of IGBT modules is indicated under multiple thermal stress levels like thermal cycling amplitudes ΔT_j and average mean temperatures T_m .

Prediction of Reliability Metrics for the Converter System

The target of this group of analyses is to map the stress behaviors of the components to the established lifetime models of component and finally acquire the reliability metrics of the components as well as the system under the specified mission profiles and converter design.

Reliability of a Single Component under Certain Mission Profiles

Most of the stress behaviors of the power electronics components translated from mission profiles fluctuate intensively in a time series. To facilitate the use of the lifetime models of components like those in Figures 14 and 15, which are normally based on fixed stress levels, some presorting and precounting methods for the stress of components are normally used. The rainflow counting [32] method, which is developed and widely used for civil and mechanical engineering, can be utilized to a certain degree in the reliability modeling of power electronics. As an example, the thermal stress shown in Figure 7 is set as an input into this algorithm, and the sorting results are shown Figure 16, in which the randomly changed thermal loadings in the time series are transferred to the amplitude ΔT_j and mean level T_m for each identified thermal cycle.

Since the stresses from ΔT_j and T_m for each thermal cycle are identified, it is possible to map them to the lifetime models of the components and acquire the time-to-failure information, if the component keeps running at this stress level. Thereby, the consumed damage D built by one of the identified thermal cycles can simply be calculated as

$$D = \frac{1}{N_{F@\text{stress}}}, \quad (4)$$

where $N_{F@\text{stress}}$ represents the number of cycles or time to failure (at a certain probability) if the component is running at the given stress level. $N_{F@\text{stress}}$ can be found from the lifetime models of components such as that shown in Figure 15.

By adding up the consumed damages from each of the identified thermal cycles in Figure 16, the total accumulated damage by the n thermal cycles $AD_{n\text{total}}$ can be calculated according to the minor rules [33]. It assumes that the damage by each of the stress cycles can be accumulated, and the total accumulated damage is always less than 1 before the component fails:

$$AD_{n\text{total}} = D_1 + D_2 + \dots + D_n < 1. \quad (5)$$

Assuming that the component is stressed by the n stress cycles repeatedly, the lifetime $L_{n\text{total}}$ when the component

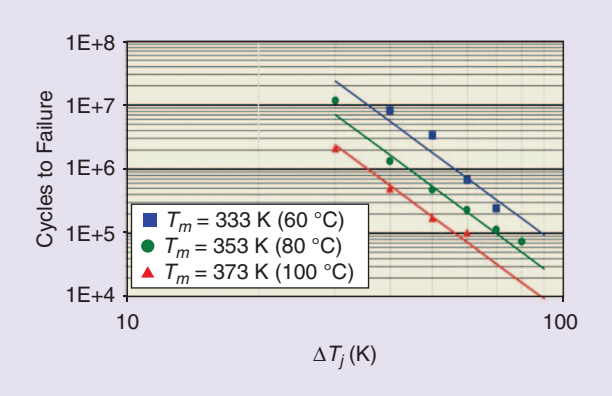


FIG 15 A strength/lifetime model tested for power semiconductor component (B10 lifetime) that is dependent on average junction temperature T_m and thermal cycling amplitude ΔT_j [25].

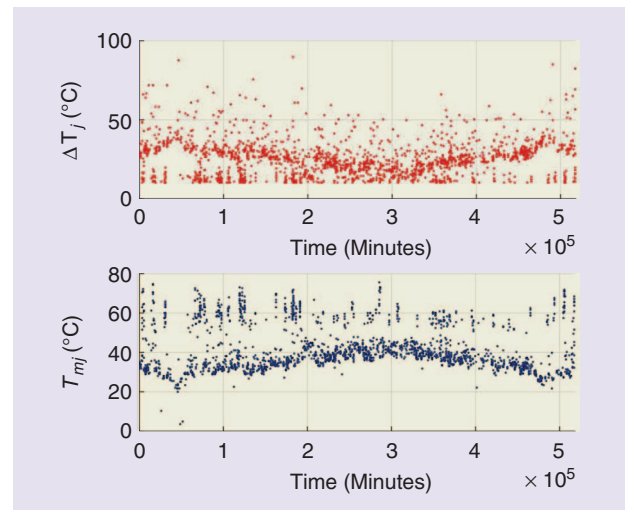


FIG 16 The rainflow sorting results for the thermal stress shown in Figure 7.

consumes 100% damage, i.e., fails at a certain probability, can be calculated as

$$L_{n\text{total}} = \frac{T_{n\text{total}}}{AD_{n\text{total}}}, \quad (6)$$

where the $T_{n\text{total}}$ represents the total time that the n stress cycles experience.

Variance of Parameters and Impacts

Besides the deterministic physics of the failure mechanisms, it is necessary to consider various variances in lifetime or reliability assessment for power electronic components and systems. The relevant sources of variances can be classified into four categories: 1) variances in environmental conditions; 2) variances in component parameters (e.g., tolerance); 3) variances in lifetime models introduced by the statistical life data analysis, as illustrated in the previous example of film capacitor testing; and 4) variances in time-dependent parameters due to component degradation.

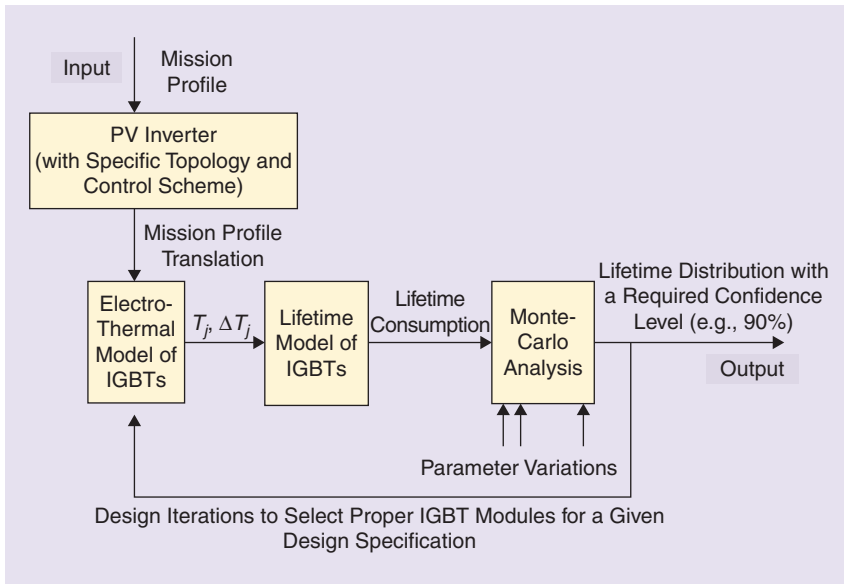


FIG 17 A Monte-Carlo-based method for lifetime prediction of IGBT bond wires [34].

To take into account the prior variances, a Monte-Carlo-based method for the lifetime prediction of an IGBT module bond wire is proposed in [34]. The flowchart of the method is shown in Figure 17, which is studied based on a photovoltaic (PV) inverter application. The IGBT bond-wire lifetime model proposed in [35] is applied

$$N_f = A \Delta T_j^\eta \left(\frac{\beta_2}{T_{j,\min}} \right) t_{\text{on}}^{\beta_2} I^{\beta_4} V^{\beta_5} D^{\beta_6}, \quad (7)$$

where ΔT_j is the junction temperature fluctuation, $T_{j,\min}$ is the minimum junction temperature, t_{on} is the heating time of the power cycling, V is the blocking voltage of the chip, D is the bond wire diameter, I is the current per wire, and A , β_1 , β_2 , β_3 , β_4 , β_5 , and β_6 are the constant parameters as discussed in [35]. Figure 18 shows the considered variances in

lifetime model parameters and an IGBT electrical parameter. By adding the variance to the parameters for reliability analysis, the lifetime of components is no longer a constant value but is distributed in a certain range. The details of the procedure and the case study can be found in [34].

Multicomponents Reliability Assessment of Converter System

After the reliability (or the curve of probabilities of surviving until a specific running time) of individual power electronics components under the given mission profiles and converter design is generated, the overall reliability of the whole converter system can be decided depending on the connection logics of the components. For the N components connected in series logic, the overall reliability $R_{N,\text{series}}(t)$ of the system can be calculated as

$$R_{N,\text{series}}(t) = \prod_{x=1}^N R_x(t), \quad (6)$$

where $R_x(t)$, which is a time-dependent variable, represents the reliability of an individual power electronics component under the given mission profiles and converter design.

For the N components connected in parallel logic, the overall reliability $R_{N,\text{parallel}}(t)$ of the system can be calculated as

$$R_{N,\text{parallel}}(t) = 1 - \prod_{x=1}^N [1 - R_x(t)]. \quad (7)$$

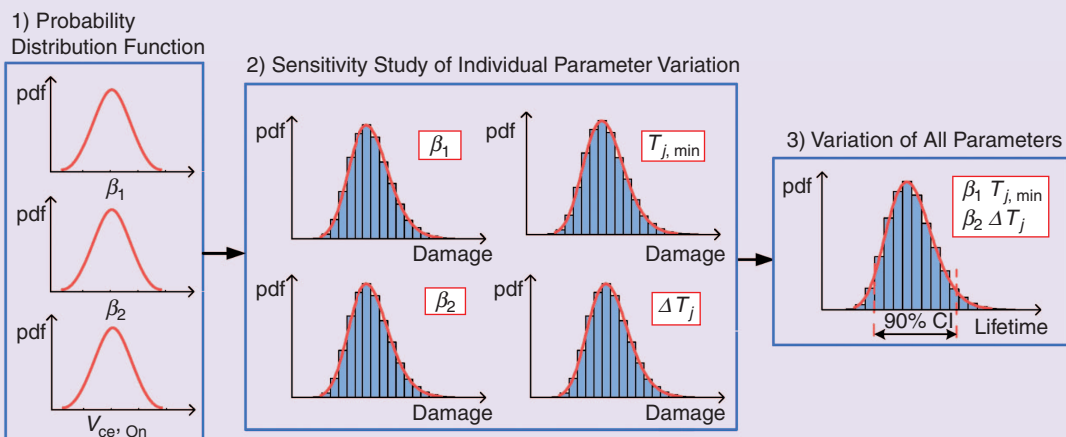


FIG 18 A step-by-step Monte-Carlo analysis of an IGBT module based on (7). β_1 and β_2 : fitting coefficients of the applied lifetime model; ΔT_j : minimum junction temperature; ΔT_j : junction temperature fluctuation; $V_{ce,\text{on}}$: collector-emitter voltage; pdf: probability distribution function [34].

In (7) it is assumed that the failure of an individual component will have no impacts to the loading and lifetime for the rest of the components in the system. However, this assumption is not always true in the power electronics converter; in this case, a more complicated calculation for the system reliability needs to be performed by taking into account the cross-impact matrix results and the repairability of the system. More details can be found in [2].

An Example Based on a Wind Power Inverter

To give a review and better understanding to the introduced approach for assessing the reliability metrics of the power electronics converter, a simple example is demonstrated on a wind power inverter, as detailed in [17].

A typical wind condition and wind turbine system are first determined as a study case. As shown in Figure 19, a one-year wind speed and ambient temperature profile is used with 3 hours averaged at an 80-m hub height, which was collected from a wind farm located near Thyborøn, Denmark, with latitude 56.71° and longitude 8.20° . The chosen hub wind speed belongs to the wind class IEC I with average wind speed of 8.5–10 minutes/seconds [35], [36], and a 2.0-MW wind turbine [37] is chosen to fit the given wind condition.

With respect to the wind power converter, the most frequently selected two-level back-to-back voltage source converter is chosen, as shown in Figure 20. Only the grid-side converter is chosen as a case study, whose parameters are designed according to Table 3, which is a state-of-the-art configuration for the two-level wind power converter. The generator-side converter can share the similar approach for the analysis.

In Figure 21, a simplified diagram for the analysis of the given inverter is shown, where multidisciplinary models like the wind turbine, generator, converter, loss, and thermal impedance of the power devices are all included to map the reliability of the device with the mission profile of the wind turbines as well as the strength model of component. Based on the given mission profiles and converter designs, the thermal loading of the power semiconductor device and the rainflow counting results have already been shown in Figures 7 and 16, respectively.

In this demonstration, the lifetime model provided by [38] is used. The total one-year consumed B10 lifetime of the IGBT module is shown in Figure 22, in which three failure mechanisms like the crack of baseplate soldering (*B* solder, caused by case temperature cycling), crack of chip soldering (*C* solder, caused by junction temperature cycling), and bond-wire lift-off (bond wire, caused by junction temperature cycling) are illustrated. The temperature cycling on the chip soldering (*C* solder) consumes more lifetime (i.e., is quicker to failure) than the other two failure mechanisms. It is worth mentioning that this lifetime result reflects only those influenced by long-term thermal cycles with a period longer than 3 hours.

The quantified reliability metrics based on the mission profiles and converter design are very useful information,

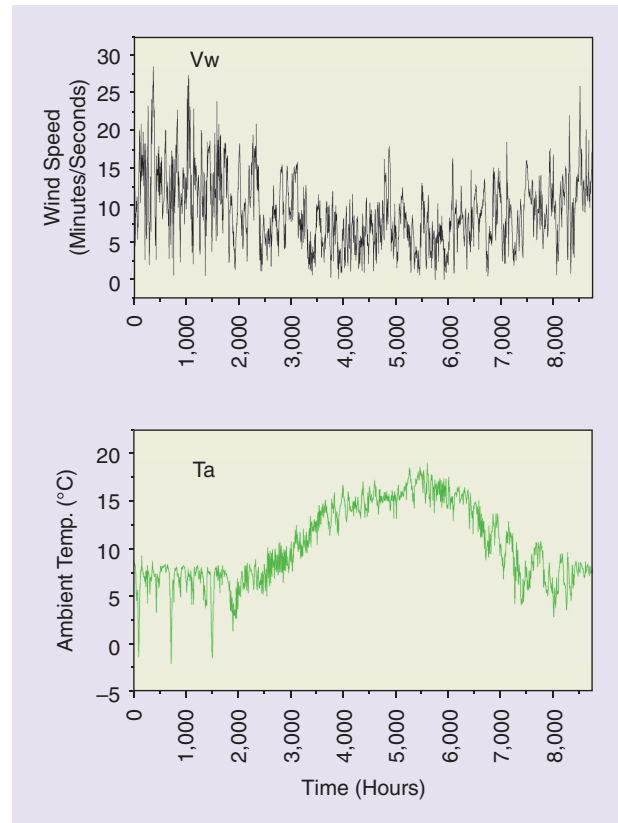


FIG 19 The one-year mission profile of wind speed and ambient temperature from a wind farm (3-hour average).

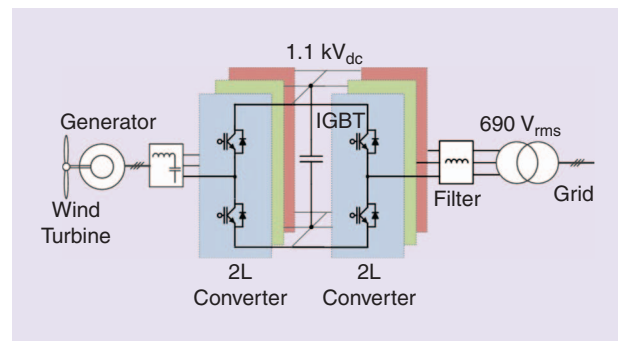


FIG 20 A wind power converter for lifetime estimation.

Table 3. The parameters of the wind power converter in Figure 20.

Rated output active power P_0	2 MW
dc bus voltage V_{dc}	1.1 kV _{dc}
*Rated primary side voltage V_p	690 V _{rms}
Rated load current	1.93 kA _{rms}
Fundamental frequency f_a	50 Hz
Switching frequency f_s	1,950 Hz
Filter inductance L_f	132 μ H [(0.2 p.u.)]

*Line-to-line voltage in the primary windings of a transformer.

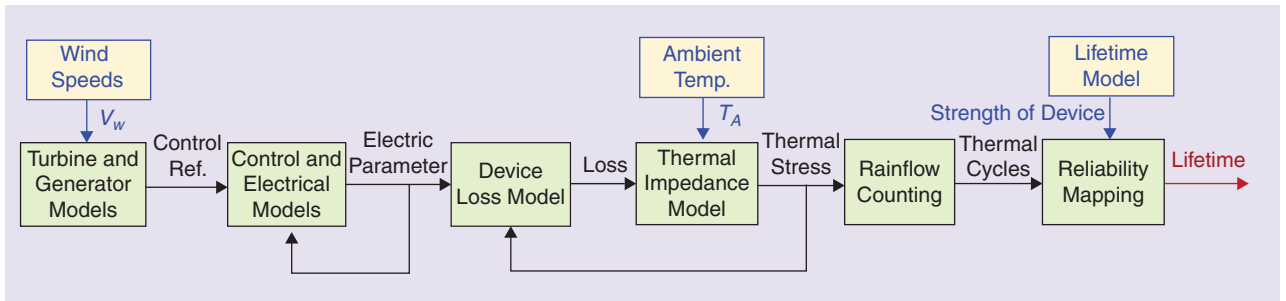


FIG 21 A flow diagram used for the lifetime prediction of power devices with the given wind power inverter and mission profiles.

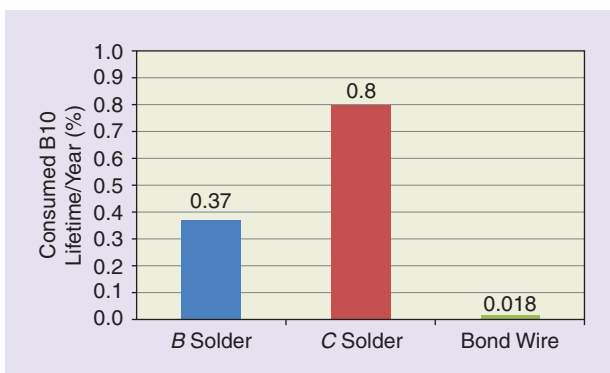


FIG 22 The consumed B10 lifetime of IGBT by long-term thermal cycles for one year (lifetime models from [38] are used, only considering thermal cycles ranging from 3 hours to one year, *B* solder means base plate solder, *C* solder means chip solder).

enabling evaluation of the influence of the converter operations/designs on the reliability performance of the system. The reliability metrics can also be used to guide the design targets and maintenance schedules of products—leading to cost reductions in energy use.

Conclusions

Reliability engineering research on power electronics is currently undergoing a paradigm shift to a more physics-of-failure approach, which provides a better understanding of failure causes and better assessment/design for the reliability performance of converter systems. However, the modeling and testing methods, as well as the analyzing tools, for power electronics need to be updated and further integrated to enable this paradigm shift. This article gives an overview of the new design flow in the reliability engineering of power electronics and discusses some of the emerging methods in this field. A new analysis flow is discussed and demonstrated, with the introduction to the multidisciplinary/multitime scale simulations, strength modeling of components, translation of mission profiles, and statistical analysis of parameters. Much more work has to be done in the future—not only on the modeling side but also in terms of testing and validation of the new methods. Finally, turning the methods into a more physics-based approach will enable a more advanced health management system of future products.

About the Authors

Ke Ma (kema@sjtu.edu.cn) received his B.Sc. and M.Sc. degrees from the Zhejiang University, China, in 2007 and 2010, respectively. He received his Ph.D. degree from Aalborg University, Denmark, in 2013, where he was an assistant professor and a work package leader with the Center of Reliable Power Electronics from 2014 to 2016. He was with Vestas Wind Systems A/S, Denmark, in 2015. In 2016, he joined the faculty of Shanghai Jiao Tong University, China, under the Thousand Talents Plan Program for Young Professionals. His research interests include the modeling and enhancement of power electronics reliability in the application of renewable energy production and motor drive systems. Since 2014, he has served as an associate editor of *IEEE Transactions on Industry Applications* and was the recipient of several prize paper awards from the IEEE. He is a Member of the IEEE.

Huai Wang (hwa@et.aau.dk) received his B.E. degree from Huazhong University of Science and Technology, Wuhan, China, in 2007 and his Ph.D. degree from City University of Hong Kong in 2012. He is currently an associate professor and a work package leader with the Center of Reliable Power Electronics, Aalborg University, Denmark. His research addresses the fundamental challenges in modeling and validation of the failure mechanisms of active and passive power electronic components and application issues in system-level predictability, circuit architecture, and robustness design. He contributed the first few concept papers in the area of power electronics reliability, filed four patents in capacitive dc-link inventions, and coedited a book. He was with the ABB Corporate Research Center, Switzerland, in 2009. He received the IEEE Power Electronics Society Richard M. Bass Outstanding Young Power Electronics Engineer Award in 2016. He has been an associate editor of *IEEE Transactions on Power Electronics* since 2015.

Frede Blaabjerg (fbl@et.aau.dk) received his Ph.D. degree from Aalborg University, Denmark. He was with ABB-Scandia, Randers, Denmark, from 1987 to 1988. His research interests include power electronics and their applications such as in wind turbines, photovoltaic systems, reliability, harmonics, and adjustable speed drives. He has received 17 IEEE prize paper awards, the IEEE Power Electronics Society Distinguished Service Award in 2009, the International Power Electronics and Motion Control Conference Council Award in 2010, the IEEE William E. Newell Power Electronics Award in 2014, and the Villum Kann Rasmussen Research Award in 2014. He

was an editor-in-chief of *IEEE Transactions on Power Electronics* from 2006 to 2012. He was nominated in 2014 and 2015 by Thomson Reuters to be among the 250 most cited researchers in engineering in the world. He is a Fellow of the IEEE.

References

- [1] H. Wang, M. Liserre, F. Blaabjerg, P. Rimmen, J. Jacobsen, T. Kvistgaard, and J. Landkildehus, "Transitioning to physics-of-failure as a reliability driver in power electronics," *IEEE Trans. Emerg. Sel. Topics Power Electron.*, vol. 2, no. 1, pp. 97–114, Mar. 2014.
- [2] P. O'Connor and A. Kleyner, *Practical Reliability Engineering*, 5th ed. West Sussex: Wiley, 2012.
- [3] H. Wang, H. Chung, F. Blaabjerg, and M. Pecht, "Reliability engineering in power electronic converter systems," in *Reliability of Power Electronic Converter Systems*, IET, 2015, ch. 1.
- [4] W. Weibull, "Statistical distribution function of wide applicability," *ASME J. Appl. Mech.*, vol. 18, no. 3, pp. 293–297, Sept. 1951.
- [5] ZVEI Robustness Validation Working Group, *Handbook for Robustness Validation of Automotive Electrical/Electronic Modules*. Frankfurt, Germany: ZVEI, 2013.
- [6] K. Ma, D. Zhou, and F. Blaabjerg, "Evaluation and design tools for the reliability of wind power converter system," *J. Power Electron.*, vol. 15, no. 5, pp. 1149–1157, 2015.
- [7] B. Hahn, M. Durstewitz, and K. Rohrig, "Reliability of wind turbines—Experience of 15 years with 1500 WTs, in *Wind Energy*. Berlin: Springer, 2007.
- [8] S. Faulstich, P. Lyding, B. Hahn, and P. Tavner, "Reliability of offshore turbines—Identifying the risk by onshore experience," presented at the European Offshore Wind, Stockholm, Sweden, 2009.
- [9] L. M. Moore and H. N. Post, "Five years of operating experience at a large, utility-scale photovoltaic generating plant," *J. Prog. Photovolt. Res. Appl.*, vol. 16, no. 3, pp. 249–259, 2008.
- [10] E. Wolfgang, "Examples for failures in power electronics systems," presented at the ECPE Tutorial on Reliability of Power Electronic Systems, Nuremberg, Germany, Apr. 2007.
- [11] S. Yang, A. T. Bryant, P. A. Mawby, D. Xiang, L. Ran, and P. Tavner, "An industry-based survey of reliability in power electronic converters," *IEEE Trans. Ind. Appl.*, vol. 47, no. 3, pp. 1441–1451, May/June 2011.
- [12] M. Ciappa, "Selected failure mechanisms of modern power modules," *Microelectron. Rel.*, vol. 42, no. 4–5, pp. 653–667, Apr.–May 2002.
- [13] H. Wang and F. Blaabjerg, "Reliability of capacitors for dc-link applications in power electronic converters—An overview," *IEEE Trans. Ind. Appl.*, vol. 50, no. 5, pp. 3569–3578, Sept.–Oct. 2014.
- [14] J. Due, S. Munk-Nielsen, and R. Nielsen, "Lifetime investigation of high power IGBT modules," in *Proc. European Conf. Power Electronics and Applications 2011*, Birmingham, U.K.
- [15] C. Busca, R. Teodorescu, F. Blaabjerg, S. Munk-Nielsen, L. Helle, T. Abeysekera, and P. Rodriguez, "An overview of the reliability prediction related aspects of high power IGBTs in wind power applications," *Microelectron. Rel.*, vol. 51, no. 9–11, pp. 1903–1907, 2011.
- [16] K. Ma and F. Blaabjerg, "Multi-timescale modelling for the loading behaviors of power electronics converter" in *Proc. IEEE Energy Conversion Congr. Exposition (ECCE)*, 2015, pp. 5749–5756.
- [17] K. Ma, M. Liserre, F. Blaabjerg, and T. Kerekes, "Thermal loading and lifetime estimation for power device considering mission profiles in wind power converter," *IEEE Trans. Power Electron.*, vol. 30, no. 2, pp. 590–602, 2015.
- [18] K. Ma, Y. Yang, and F. Blaabjerg, "Transient modelling of loss and thermal dynamics in power semiconductor devices" in *Proc. IEEE Energy Conversion Congr. Exposition (ECCE)*, Nov. 2014, pp. 5495–5510.
- [19] A. Bahman, K. Ma, P. Ghimire, F. Iannuzzo, and F. Blaabjerg, "A 3D lumped thermal network model for long-term load profiles analysis in high power IGBT modules," *IEEE J. Emerg. Sel. Topics Power Electron.*, vol. 4, no. 3, pp. 1050–1063, 2016.
- [20] K. Ma, N. He, M. Liserre, and F. Blaabjerg, "Frequency-domain thermal modelling and characterization of power semiconductor devices," *IEEE Trans. Power Electron.*, vol. 31, no. 10, pp. 7183–7193, 2016.
- [21] W. B. Nelson, *Accelerated Testing—Statistical Models, Test Plans, and Data Analysis*. Hoboken, NJ: Wiley, 2004.
- [22] General Motors Corporation Handbook GMW8758. *Calibrated Accelerated Life Testing*, 2004.
- [23] K. Bhote and A. Bhote, *World Class Reliability: Using Multiple Environment Overstress Tests to Make It Happen*. New York, NY: AMACOM, 2004.
- [24] G. K. Hobbs, *Accelerated Reliability Engineering: HALT and HASS*. New York: Wiley, 2000.
- [25] M. Held, P. Jacob, G. Nicoletti, P. Scacco, and M. H. Poech, "Fast power cycling test for IGBT modules in traction application," in *Proc. Power Electronics and Drive Systems*, 1997, pp. 425–430.
- [26] H. Berg and E. Wolfgang, "Advanced IGBT modules for railway traction applications: Reliability testing," *Microelectron. Rel.*, vol. 38, no. 6–8, pp. 1319–1323, June–Aug., 1998.
- [27] V. Smet, V. F. Forest, and J. Huselstein, "Ageing and failure modes of IGBT modules in high-temperature power cycling," *IEEE Trans. Ind. Electron.*, vol. 58, no. 10, pp. 4931–4941, Oct. 2011.
- [28] A. Hutzler, F. Zeyss, S. Vater, and L. M. Maerz, "Power cycling community 1995–2014—An overview of test results over the last 20 years," *Bodo's Power Systems*, no. 05–14, pp. 78–81, May 2014.
- [29] P. Ghimire, "Real time monitoring and wear out of power modules," Ph.D. dissertation, Aalborg Univ., Denmark, Sept. 2015.
- [30] U. Choi, S. Jørgensen, and F. Blaabjerg, "Advanced accelerated power cycling test for reliability investigation of power device modules," *IEEE Trans. Power Electron.*, vol. 31, no. 12, pp. 8371–8386, Dec. 2016.
- [31] H. Wang, P. Reigosa, and F. Blaabjerg, "A humidity-dependent lifetime derating factor for DC film capacitors" in *Proc. IEEE Energy Conversion Congr. and Exposition*, Sept. 2015, pp. 3064–3068.
- [32] A. Nieslony, "Determination of fragments of multiaxial service loading strongly influencing the fatigue of machine components," *Mech. Syst. Signal Process.*, vol. 23, no. 8, pp. 2712–2721, 2009.
- [33] M. A. Miner, "Cumulative damage in fatigue," *J. Appl. Mech.*, vol. 12, pp. A159–A164, 1945.
- [34] P. D. Reigosa, H. Wang, Y. Yang, and F. Blaabjerg, "Prediction of bond wire fatigue of IGBTs in a PV inverter under a long-term operation," *IEEE Trans. Power Electron.*, vol. 31, no. 10, pp. 7171–7182, Oct. 2016.
- [35] R. Bayerer, T. Hermann, T. Licht, J. Lutz, and M. Feller, "Model for power cycling lifetime of IGBT Modules—Various factors influencing lifetime," presented at the Int. Conf. Integrated Power Systems (CIPS), Nuremberg, Germany, 2008.
- [36] Wikipedia. (June 2013). IEC 61400. [Online]. Available: http://en.wikipedia.org/wiki/IEC_61400#cite_note-woeb-1
- [37] Vestas Wind Power. (June 2013). Wind turbines classes. [Online]. Available: <http://www.vestas.com/>
- [38] J. Berner, "Load-cycling capability of HiPak IGBT modules," ABB Application Note 5SYA 2043-02, 2012.

